Relationships between Lower Limb Muscle Characteristics and Force–Velocity Profiles Derived during Sprinting and Jumping

PHILLIP BELLINGER[1,2], MATTHEW N. BOURNE[1,3], STEVEN DUHIG[1,3], ELINE LIEVENS[4], BEN KENNEDY[5], ANDREW MARTIN[1], CHRISTOPHER COOPER[1], MATTHEW TREDREA[6], HAL RICE[5], WIM DERAVE[4], and CLARE MINAHAN[1]

[1]Griffith Sports Science, Griffith University, Gold Coast, Southport, Queensland, AUSTRALIA; [2]Queensland Academy of Sport, Queensland, AUSTRALIA; [3]Gold Coast Centre for Orthopaedics Research, Engineering and Education (GCORE), Menzies Health Institute Queensland, Griffith University, Southport, Queensland, AUSTRALIA; [4]Department of Movement and Sports Sciences, Ghent University, Ghent, BELGIUM; [5]Qscan Radiology, Queensland, AUSTRALIA; and [6]Department of Rehabilitation, Nutrition and Sport, La Trobe University College of Science Health and Engineering, Nutrition and Sport, Bundoora, AUSTRALIA

ABSTRACT

BELLINGER, P., M. N. BOURNE, S. DUHIG, E. LIEVENS, B. KENNEDY, A. MARTIN, C. COOPER, M. TREDREA, H. RICE, W. DERAVE, and C. MINAHAN. Relationships between Lower Limb Muscle Characteristics and Force–Velocity Profiles Derived during Sprinting and Jumping. *Med. Sci. Sports Exerc.*, Vol. 53, No. 7, pp. 1400–1411, 2021. **Purpose:** This study aimed to identify the relationships between lower limb muscle characteristics and mechanical variables derived from the vertical (jumping) and horizontal (sprinting) force–velocity–power (FVP) profiles. **Methods:** Nineteen subelite male rugby league players performed a series of squat jumps and linear 30-m sprints to derive the vertical and horizontal FVP profiles, respectively. The theoretical maximal force (F_0), velocity (V_0), and power (P_{max}) were derived from both the vertical (i.e., vF_0, vV_0, and vP_{max}) and the horizontal (i.e., hF_0, hV_0, and hP_{max}) FVP profiles. Vastus lateralis (VL), biceps femoris long head, and gastrocnemius medialis (GM) and lateralis muscle fascicle length, pennation angle, and thickness were measured using B-mode ultrasonography. Magnetic resonance imaging was used to calculate volumes of major lower limb muscles, whereas proton magnetic resonance spectroscopy was used to quantify the carnosine content of the GM to estimate muscle fiber typology. **Results:** Variation in vP_{max} was best explained by GM muscle fiber typology (i.e., greater estimated proportion of Type II fibers) and VL volume (adjusted $r^2 = 0.440$, $P = 0.006$), whereas adductor and vastus medialis volume and GM muscle fiber typology explained the most variation in hP_{max} (adjusted $r^2 = 0.634$, $P = 0.032$). Rectus femoris and VL volume explained variation in vF_0 ($r^2 = 0.430$, $P = 0.008$), whereas adductor and vastus medialis volume explained variation in hF_0 ($r^2 = 0.432$, $P = 0.007$). Variations in vV_0 and hV_0 were best explained by GM muscle fiber typology (adjusted $r^2 = 0.580$, $P < 0.001$) and GM muscle fiber typology and biceps femoris short head volume (adjusted $r^2 = 0.590$, $P < 0.001$), respectively. **Conclusion:** Muscle fiber typology and muscle volume are strong determinants of maximal muscle power in jumping and sprinting by influencing the velocity- and force-oriented mechanical variables. **Key Words:** MUSCLE FIBER–TYPE COMPOSITION, MUSCLE FASCICLE LENGTH, MUSCLE VOLUME, CARNOSINE, JUMP PERFORMANCE, SPRINT PERFORMANCE

APPLIED SCIENCES

Generating a large amount of force at a high-contraction (or movement) velocity is critical for many "explosive" movements and is a key performance variable in many sports (1). Indeed, for the sport of rugby league, lower limb maximal muscle power is one of the strongest discriminatory performance variables that differentiates between elite National Rugby League (NRL) players and their second-division counterparts (2). Given that maximal muscle power is directly influenced by the underlying force and velocity mechanical outputs, the force–velocity (FV) and power–velocity (PV) relationships have been used to profile the theoretical maximal mechanical output during sprinting and jumping activities (3,4). The assessment of the FV and PV relationships during these movements characterizes the external force production capabilities of the lower limbs by identifying the theoretical maximum force (F_0), velocity (V_0), and power (P_{max}) produced during sprinting (i.e., horizontal; hF_0, hV_0, and hP_{max}) or jumping (i.e., vertical; vF_0, vV_0, and vP_{max}) (3,5). Although these mechanical capabilities are clearly important for sprinting and jumping performance, the lower limb muscle characteristics underpinning these mechanical capabilities are yet to be fully elucidated.

The external force production capabilities of the lower limbs are likely to be influenced by several muscle characteristics, including muscle architecture (i.e., fascicle length, pennation

Address for correspondence: Phillip Bellinger, Ph.D., School of Allied Health Sciences, Griffith University, Southport, QLD 4222, Australia; E-mail: p.bellinger@griffith.edu.au.
Submitted for publication August 2020.
Accepted for publication December 2020.

0195-9131/21/5307-1400/0
MEDICINE & SCIENCE IN SPORTS & EXERCISE®

DOI: 10.1249/MSS.0000000000002605

angle, and thickness), morphology (i.e., muscle volume), and the distribution of Type I and Type II muscle fibers (i.e., fiber typology). Muscle fiber typology is largely dependent on genetic predisposition, and the transition between Type I and Type II fibers is not thought to occur very readily in response to training (6). By contrast, muscle volume and architecture are more malleable to training, and changes in these characteristics can occur quite rapidly (7). Although interindividual differences in the FV profile have previously been used to individualize training prescription (8), a better understanding of the muscle characteristics that modulate this profile may improve our ability to prescribe performance-enhancing exercise interventions. For example, identifying the extent to which muscle architecture and volume contribute to the external force production capabilities may inform the design of training interventions that preferentially target adaptations in these characteristics, thus maximizing the training response. Furthermore, greater insight into how muscle fiber typology contributes to the external force production capabilities of the lower limbs may influence the interpretation of the FV profile for individualizing training programs (8). Interestingly, in high-level athletes, there are trivial to small correlations between the maximal mechanical variables derived from vertical and horizontal FV and PV profiles (9). That is, an athlete who can produce a large vF_0 does not necessarily have the capacity to produce an equally high hF_0. Although this divergence might be partly explained by differences in force orientation ability between sprinting and jumping, it also suggests that the muscular characteristics underpinning the mechanical variables derived from horizontal and vertical FV and PV profiles are likely to differ significantly.

Although few studies have determined the muscular characteristics that underpin the maximal mechanical parameters of the vertical and horizontal FV and PV profiles, the associations between muscle characteristics and performance metrics (i.e., sprint times or jump height) and/or levels of performance (i.e., trained and untrained) have been reported (10–18). For example, previous research has reported a significant correlation ($r = -0.69$) between the proportion of Type II muscle fibers and 100-m sprint time (15) and the squat jump mean mechanical power (19), suggesting that muscle fiber typology may influence the external force production capabilities of the lower limbs. Muscle architecture may also influence the FV and the PV mechanical parameters given that muscles with longer fascicles possess greater shortening velocity (20). Furthermore, elite 100-m sprinters (10.0–10.9 s) display longer fascicles in the vastus lateralis (VL) and the gastrocnemius medialis (GM) and gastrocnemius lateralis (GL) compared with their subelite counterparts (11.0–11.7 s) (14) and distance runners (10). Recent work (21) reported that GM muscle fascicle length accounted for almost half of the difference in plantarflexion V_0 between young and old men, whereas quadriceps thickness and VL pennation angle explained ~62% of the variation in countermovement jump vF_0 (22). Given that an increase in fiber pennation angle presumably result in an increase in the number of sarcomeres in parallel, and a larger physiological cross-sectional area (CSA), it could also be expected that this would result in a larger force-generating capacity (20).

Most hip- and knee-crossing muscles are significantly larger in sprinters and long jumpers compared with recreationally active individuals (11,18,23) and endurance runners (12), and total thigh muscle volume is associated with faster 5-m sprint times and greater squat jump power output (13). It could be postulated that the longer ground contact times during the early phase of sprint running allows the time for higher levels of muscle force to be produced. Thus, muscle characteristics, such as volume, that directly influence maximal muscle force are likely to affect F_0. Specifically, the adductors (ADD) provide a major contribution to hip extension torque during the late-swing to early contact phase of sprint acceleration (24), whereas knee flexor and extensor torque is thought to contribute to the swing and stance phases during sprinting (25). Despite these observations, the associations between lower limb muscle characteristics and maximal mechanical parameters that underpin sprint running and jumping performance have not been studied.

The primary aim of the present study was to determine the influence that lower limb muscle architecture, morphology, and fiber typology have on the maximal mechanical parameters of the FV and PV profiles derived during sprinting and jumping in subelite rugby league players. We hypothesized that (i) muscle fiber typology (greater estimated proportion of Type II fibers) would be positively associated with vV_0, hV_0, vP_{max} and hP_{max}; (ii) the fascicle length of lower limb muscles would be associated with hV_0 and hP_{max} whereas the fascicle length of the VL would be associated with vV_0 and vP_{max}; (iii) the volume of most hip and knee-crossing muscles, but not ankle-crossing muscles, would be positively associated with hF_0 and hP_{max}; and (iv) the volume of knee extensor muscles as well as the angle of pennation and muscle thickness of the VL would be positively associated with vF_0 and vP_{max}.

METHODOLOGY

Participants. Nineteen male rugby league players (age = 19.2 ± 0.7 yr, stature = 180.7 ± 5.6 cm, body mass = 89.9 ± 10.0 kg) participated in the current study. The players were from the same elite youth development system within an Australian NRL club. All players were involved in full training and competition and had no history of lower limb injury within 12 months of testing and had at least 4 yr of experience in resistance training. All players provided written informed consent before participating in this study, which was approved by the Griffith University Human Research Ethics Committee.

Study design. Data collection was conducted during a 4-d testing period after the 2019 NRL preseason. Participants had a week of reduced training load after the completion of the preseason preparation period as the team had a bye in the first round of competition and the testing was completed at the end of this week. Participants underwent magnetic resonance imaging (MRI) of their entire lower limb to determine volumes

of the major hip, knee, and ankle-spanning muscles and proton magnetic resonance spectroscopy (^{1}H-MRS) of the GM to estimate muscle fiber typology (26). In addition, the muscle architecture of the biceps femoris long head (BFLH), VL, and GM and GL was assessed via two-dimensional (2D) ultrasound. Figure 1 displays an overview of these measurements. Subsequently, each participant performed one session of maximal squat jumps with additional loads of 10%–100% of their body mass to determine the mechanical parameters associated with the vertical FV profile. In a separate session 48 h later, each participant performed maximal 30-m sprints to determine the mechanical parameters associated with the horizontal FV profile using a validated biomechanical model (3).

FV relationship during the squat jump. Each participant completed a 20-min general warm-up consisting of jogging and joint mobility exercises, which was followed by a specific warm-up comprising several trials of both unloaded and loaded squat jumps. Participants performed maximal unloaded (without external load) and loaded (external loads ranging from 10% to 100% body mass) squat jumps to determine the individual FV and PV relationships (4). For each squat jump, participants were instructed to stand up straight and still on the center of a bilateral force plate (ForceDecks; Vald Performance, Queensland, Australia) with a dowel rod (unloaded trials) or barbell (loaded trial) placed on their upper trapezius. External loads were added in sequential order until jump height fell below 15 cm. All subjects performed squat jumps with at least a load of 60% body mass until jump height fell below 15 cm. For each squat jump, participants were asked to flex their hips and knees while keeping their spine neutral, reach the starting squat height (~90° knee angle) and pause for a count of 2 s, before applying as much voluntary force into the ground as possible and jumping for maximum height. Countermovement was forbidden, carefully checked, and confirmed by the force plate technology. Two valid trials were performed with each load with a 4-min recovery between different loads and trials.

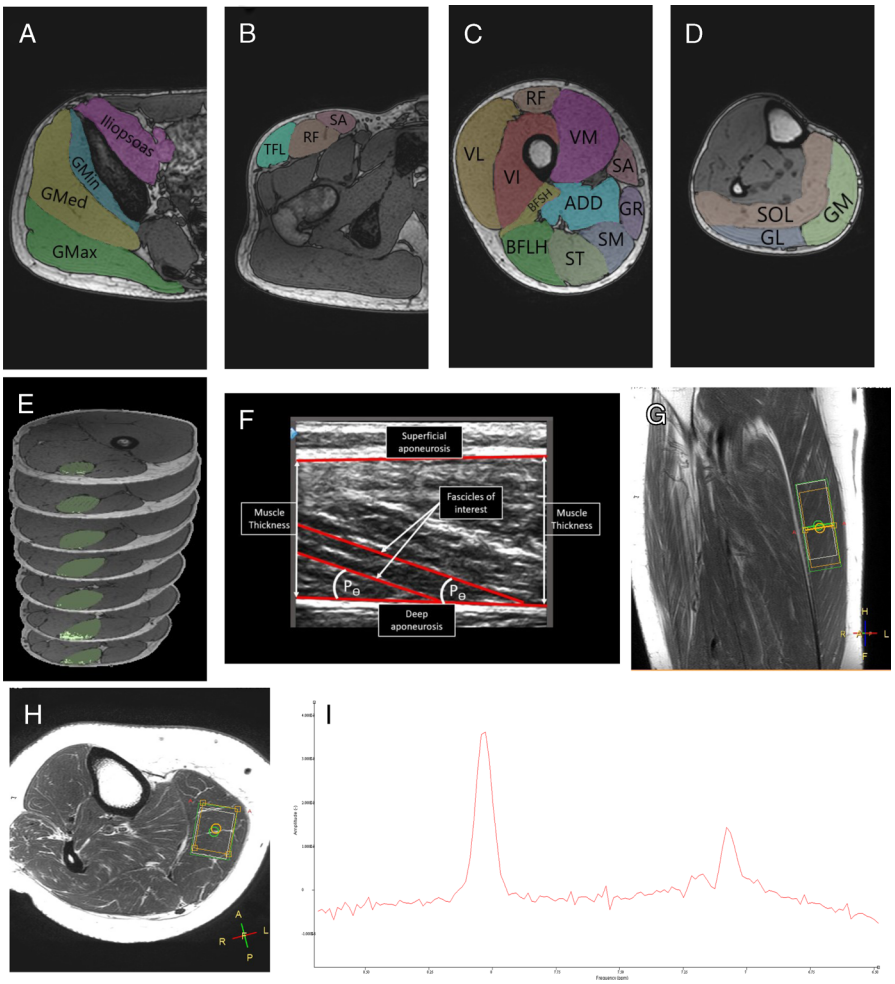

FIGURE 1—Participants underwent MRI of their entire lower limb to determine muscle volumes of the major hip, knee, and ankle-spanning muscles. Muscles were segmented in axial MR images from the hip (A and B), the thigh (C), and the shank (D). Muscle volume was calculated by multiplying the interslice distance by the sum of the CSA of the total number of traced slices (E; semitendinosus). Muscle thickness, fascicle pennation angle, and fascicle length were measured by B-mode ultrasonography of the VL, BFLH, and GL and GM (F). We also used proton MR spectroscopy (^{1}H-MRS) to quantify the carnosine content in the GM to estimate muscle fiber typology. Panels G and H show a coronal and transverse MR image to demonstrate the localization of the voxel, and panel I shows a detailed spectra of the downfield carnosine region. ADD, adductor magnus, longus, and brevis; SA, sartorius; GR, gracilis; SM, semimembranosus; ST, semitendinosus; SOL, soleus.

The force plates had a sampling rate of 1000 Hz, and commercially available ForceDecks software (Vald Performance) was used to analyze all squat jumps. The mean force, power, and velocity were extracted from each loading condition during the concentric phase, which was defined as the sample immediately before a 20-N change above the measured mass until the time point at which total vertical force fell under the threshold of 20 N below mass. The FV and the PV relationships were constructed by plotting mean force and mean velocity using linear regression, whereas mean power and mean velocity were plotted using second-degree polynomial functions. vF_0 and vV_0 were then identified from the FV relationship as the *x*- and *y*-intercepts, respectively, whereas vP_{max} was determined as the apex of the PV relationship (27). In our laboratory, vF_0, vV_0, and vP_{max} have coefficient of variation (CV) values of 3.8%, 5.4%, and 6.8%, respectively.

FV relationship during sprinting. All sprint testing was completed on the same well-maintained natural grass surface, and all participants wore studded training shoes and training attire. Each participant performed a 15-min on-field dynamic warm-up protocol, which closely reflected the warm-up used before field-based training sessions. Participants performed two linear 30-m sprints, and sprint times were recorded by infrared timing gates (Smartspeed, Fusion Sport, Australia) with split times every 5 m. All starts commenced from a static position, and the upper body of each participant was positioned as close as possible to the intergate beam of the first timing gate, which was placed on the starting line. The timing gates at the start line and 5 m line were mounted on separate tripods 1.00/1.20 m above the ground level, whereas the remaining gates were mounted 1.30/1.50 m above the ground level. Based on available correction factors (28), we added 0.5 s to all sprint times to ensure that the start time initiation was likely to coincide with the first rise of the force production onto the ground. We computed individual PV and FV profiles using the validated biomechanical model proposed by Samozino et al. (3), which have been shown to have high reliability (CV and standard error of measurement <5%). In brief, we used the changes in running velocity over time to compute the acceleration of each participant's center of mass in the anteroposterior direction and then used the aerodynamic friction of force and each athlete's body mass and stature to estimate the net horizontal ground reaction force. hF_0 and hV_0 were then identified from the FV relationship as the *x*- and *y*-intercepts, respectively, and hP_{max} was determined as the apex of the PV relationship. We used the mean of the mechanical variables calculated from each of the two sprints to reduce the typical error associated with using a single sprint (28).

Carnosine quantification via ^{1}H-MRS. Muscle carnosine content was measured by ^{1}H-MRS in the GM of each participant's right limb to estimate muscle fiber typology. We chose to estimate the muscle fiber typology of the GM because (i) we can measure carnosine reliably in this muscle, (ii) carnosine content in the GM muscle has been positively correlated with the percentage area occupied by Type II muscle fibers (26), and (iii) the GM makes a substantial contribution to force and power production during running and jumping (29,30). This suggests that the fiber composition of the GM may be meaningful in the context of sprinting and jumping. ^{1}H-MRS measurements were performed on a 3-T whole body MRI scanner (Philips Medical Systems Best, The Netherlands). Participants were lying in a supine position, while their lower leg was fixed in a spherical knee-coil. All the spectra were acquired using a single-voxel point-resolved spectroscopy with the following parameters: repetition time, 2000 ms; echo time, ~40 ms; number of excitations, 128 (carnosine) and 16 (water); spectral bandwidth, 2048 Hz; and acquisition time, 4 min 16 s (carnosine) and 32 s (water). The voxel size was 40 × 15 × 20 mm. Spectral data analysis was carried out using jMRUI (version 6.0), with carnosine peaks fitted and expressed relative to the internal water signal.

Carnosine content (mM) was calculated using following formula:

$$\mathrm{Cm} = \frac{(\mathrm{CS})}{\mathrm{H_2O_s}} \times \frac{\mathrm{H_2O_{T1r}}}{\mathrm{CT_{1r}}} \times \frac{\mathrm{H_2O_{T2r}}}{\mathrm{CT_{2r}}} \times \mathrm{H_2O_{muscle}} \times \mathrm{H_2O_{protons}} \quad [1]$$

where Cm is the carnosine concentration; C_S is the carnosine signal; H_2O_S is the water signal; C_{T1r}, C_{T2r}, H_2O_{T1r}, and H_2O_{T2r} are the relaxation correction factors for carnosine (earlier described by Baguet et al. [26]) and water (earlier described by MacMillan et al. [31]); H_2O_{muscle} is the concentration of water in muscle, which was deducted from the molar concentration of water (55,000 mM) and the approximate water content of skeletal muscle tissue (0.7 $L \cdot kg^{-1}$ wet weight of tissue); and H_2O_{proton} is the number of protons in water. The CV for test–retest interday carnosine measurements in our laboratory was 4.3% (n = 15 participants) (32). In the present study, the carnosine concentration was converted to a *z*-score based on the normal distribution of our reference population. The absolute value of the *z*-score represents the distance between the individual value of a participant and the reference population mean value in units of the SD. The reference sample population consisted of 40 recreationally active male subjects (age = 22.4 ± 2.1 yr, height = 176.1 ± 17.2 cm, body mass = 81.2 ± 11.9 kg) who were scanned in our laboratory in the past 12 months.

Two-dimensional ultrasound imaging. Muscle architecture was measured *in vivo* using 2D B-mode ultrasonography (frequency = 7 MHz, depth = 50 mm, field of view = 10 × 39 mm) (Echo Blaster 128 CEXT; Telemed Medical Systems, Milan, Italy). Bilateral muscle assessments included VL (50% distance between greater trochanter and lateral femoral condyle) (14), BFLH (50% distance between ischial tuberosity and popliteal fold in the line of action of the BF) (33), GL (30% proximal distance between the lateral tibial condyle and the lateral malleolus in the midline of the muscle), and GM (at the same distance as GL, transferred medially, from the midline of the muscle) (14). All images were taken in the longitudinal axis with the participant laying prone for GM, GL, and BF measures and supine for VL. Images were acquired after a period of at least 5 min of inactivity. To capture images, the ultrasound transducer was placed perpendicular to the surface of the skin, parallel with the presumed fascicle angle at the

aforementioned sites. The transducer was then moved accordingly so that both superficial and deep aponeuroses were aligned in parallel on the viewing screen. Water-soluble conductive gel was placed on the transducer surface to enhance image quality while minimal pressure was placed on the skin surface to ensure no muscle distortion and maintain image quality. Two images were captured at each site bilaterally with the highest-quality image of the two used for analyses. Image analysis was completed offline using publicly available software (ImageJ 1.52n; National Institutes of Health, Bethesda, MD). Muscle thickness was determined as the average distance between superficial and intermediate aponeuroses at the left and right extremity of each image. Subsequently, two fascicles of interest were outlined in each image, and the mean angle between each fascicle and the deep aponeurosis was determined as the pennation angle. Given that the entire fascicle was not always visible in the field of view, fascicle length was estimated using a previously validated equation (34) (fascicle length = muscle thickness × [sin (pennation angle)]$^{-1}$). Intraclass correlation (ICC) and CV were 0.99–1.00 and 2.5%–3.0% for muscle thickness, 0.96–0.97 and 4.4%–5.5% for pennation angle, and 0.96–0.98 and 4.4%–5.4% for fascicle length. For each muscle architecture measure, we used the mean of the right and left leg for all analyses given that there were no significant differences in individual muscles from either limb.

Muscle volume. Axial T1-weighted 3D fast field echo sequences were acquired using a 3-T MRI scanner (Philips Medical Systems) from the level of the iliac crest to the ankle spanning both legs while the participant lay supine in the scanner. The images were acquired in five stations with ~210 slices per station and 10 mm overlap between stations. Slice thickness was 2.0 mm, interslice gap was 0.0 mm, repetition time was 4.1 ms, echo time 1 was 1.44 ms, and echo time 2 was 2.6 ms. The CSA values of lower limb muscles or muscle groups of both legs were determined at predefined lengths of 20%, 30%, 40%, 50%, 60%, 70%, and 80% of the total muscle length by manually tracing the margin of the respective muscle in the relevant axial slices using image analysis software (Mimics, version 17; Materialize). The analyzed muscles were the gluteus maximus (GMAX), medius (GMED), and minimus (GMIN); tensor fascia latae (TFL); sartorius; iliopsoas; gracilis; adductor magnus, longus, and brevis; rectus femoris (RF); VL; vastus intermedius (VI); vastus medialis (VM); semimembranosus; semitendinosus; BFLH; BF short head (BFSH); soleus; GM; and GL. The identification of the borders between adductor magnus, longus, and brevis was difficult; therefore, these muscles were analyzed as a muscle group and referred to as ADD. All segmentations were performed by two members of the research team. Muscle volume was calculated under the assumption that the muscle is an ideal cylinder whereby the known distance between slices was multiplied by the sum of the CSA of the total number of traced slices. This methodology (i.e., using eight slices) has been shown to have high levels of agreement (i.e., differences of <0.005%) with muscle volume calculations using 50 slices (35). To reduce the effects of body size on muscle size differences, we normalized muscle volume by stature and the product of height and body mass (11). For each muscle volume, we used the mean of the right and left leg for all analyses given that there were no significant differences in the muscle volume of individual muscles from either limb. The interrater reliability of the normalized muscle volume of the semitendinosus, semimembranosus, BFLH, BFSH, gracilis, ADD, GMAX, GMED, and GMIN was extremely good (mean ICC = 0.973, CV = 2.0%). We expressed the sum of all individual muscle volumes as total muscle volume.

Statistical analysis. Values are expressed as mean ± SD. We first performed univariable linear regression analyses to identify the muscle characteristics that were significantly associated with the mechanical variables of the vertical and horizontal FV and PV relationships, which allowed us to test our different hypotheses. After this, we performed stepwise linear regression to identify the best combination of muscle characteristics that explained the most variation in the mechanical variables. To reduce the number of comparisons in the stepwise regression models, we only included muscle characteristics in the analysis if a significant r value ($P < 0.05$) was identified with the given mechanical variable from the univariable analyses. Statistical software was used for analysis (Statistical Package for the Social Sciences for Windows, version 26.0; SPSS Inc., Chicago, IL).

RESULTS

Horizontal FV and PV profiles. Table 1 shows the mean mechanical variables from the horizontal FV and PV profiles, as well as the 5- and 30-m sprint times, whereas Table 2 shows the lower limb muscle architecture, morphology, and fiber typology values. Univariable analyses indicated that the muscle volumes of GMAX, ADD, RF, VM, VI, sartorius, and iliopsoas; the thickness of GL and GM; and the GM pennation angle were all positively associated with hF_0 (N·kg^{-1}; r = 0.431–0.579, $P < 0.05$; Table 3). Muscle volumes of the BFSH, ADD, and VM, in addition to BFLH fascicle length, and GM carnosine z-score were all significantly positively associated with hV_0 (m·s^{-1}; r = 0.513–0.678, $P < 0.05$). hP_{max} (W·kg^{-1}) was significantly positively associated with the muscle volumes of BFLH, ADD, RF, VM, VI, TFL, sartorius, and iliopsoas, as well as GM carnosine z-score and BFLH fascicle length (r = 0.485–0.669, $P < 0.05$).

Figure 2 and Table 4 show the results of the multiple linear regression models demonstrating the combination of muscle characteristics that explained the greatest variation in horizontal FV and PV mechanical variables. Variation in hF_0 (N·kg^{-1}) was best explained by the combination of ADD and VM muscle volume (adjusted r^2 = 0.432, P = 0.007), whereas variation in hV_0 (m·s^{-1}) was best explained by the combination of GM carnosine z-score and BFSH muscle volume (adjusted r^2 = 0.590, $P < 0.001$). Variation in hP_{max} (W·kg^{-1}) was best explained by a three-parameter model, including the combination of GM carnosine z-score and ADD and VI muscle volume (adjusted r^2 = 0.634, P = 0.032). The standardized beta coefficients for each regression model suggested that each muscle

TABLE 1. Mechanical variables derived from the vertical (i.e., v) and horizontal (i.e., h) FV and PV relationship as well as 5- and 30-m sprint times and jump height.

Variable	Mean ± SD	Range
Absolute hF_0 (N)	654 ± 114	468–882
Relative hF_0 (N·kg^{-1})	7.53 ± 0.81	6.14–9.14
hV_0 (m·s^{-1})	8.70 ± 0.50	8.07–9.95
Absolute hP_{max} (W)	1536 ± 226	1201–1976
Relative hP_{max} (W·kg^{-1})	17.6 ± 1.63	14.8–21.7
5-m sprint time (s)	1.35 ± 0.07	1.24–1.48
30-m sprint time (s)	4.49 ± 0.15	4.22–4.73
Absolute vF_0 (N)	3028 ± 344	2428–3658
Relative vF_0 (N·kg^{-1})	35.0 ± 3.43	29.0–40.2
vV_0 (m·s^{-1})	2.39 ± 0.31	1.95–3.00
Absolute vP_{max} (W)	1822 ± 250	1487–2389
Relative vP_{max} (W·kg^{-1})	20.8 ± 1.94	17.6–24.4
Jump height (cm)	32.2 ± 3.95	25.2–43.0

hF_0, maximum horizontal force; hV_0, maximum horizontal velocity; hP_{max}, maximum horizontal power; vF_0, maximum vertical force; vV_0, maximum vertical velocity; vP_{max}, maximum vertical power.

characteristic included in each model exerted a similar influence on the given mechanical parameter. Figure 3 shows typical traces of horizontal FV and PV relationships for subjects with similar lower limb muscle volume but divergent in muscle fiber typology (Fig. 3A, subjects A and B) and for subjects with similar muscle fiber typology but divergent in lower limb muscle volume (Fig. 3B, subjects C and D).

Vertical FV and PV profiles. Table 1 shows the mean mechanical variables from the vertical FV and PV profiles as well as jump height. Univariable analyses indicated that the muscle volumes of the ADD, RF, VL, VI, and GM thickness were all significantly positively associated with vF_0 (r = 0.479–0.548, $P < 0.05$; Table 3). GL pennation angle and GM carnosine z-score were significantly positively associated with vV_0 (r = 0.493–0.762, $P < 0.05$). vP_{max} was significantly positively associated with the muscle volume of the VL as well as the GM carnosine z-score (r = 0.581–0.647, $P < 0.01$; Table 3).

Figure 2 and Table 4 show the results of the multiple linear regression models demonstrating the combination of muscle characteristics that explained the greatest variation in vertical FV and PV mechanical variables. Variation in vF_0 was best explained by RF and VL muscle volume (r^2 = 0.430, P = 0.008), whereas variation in vV_0 was best explained by variation in GM carnosine z-score (r^2 = 0.580, $P < 0.001$). Variation in vP_{max} was most associated with the variation in GM z-score and VL muscle volume (r^2 = 0.440, P = 0.006). The standardized beta coefficients for each regression model suggested that each muscle characteristic included in each model exerted a similar influence on the mechanical parameter.

DISCUSSION

As far as the authors are aware, this is the first study to use noninvasive techniques to explore the underpining muscle characteristics of the horizontal and vertical FV and PV relationships during sprinting and jumping. The key findings are as follows: (i) higher GM carnosine z-score (i.e., greater estimated proportion of Type II fibers) was associated with greater vV_0, hV_0, vP_{max}, and hP_{max} values, and (ii) greater knee extensor muscle volume was associated with higher vF_0 and vP_{max}, and ADD and knee extensor volume contributed to the explained variation in hF_0 and hP_{max}. These findings suggest that muscle fiber typology is a key determinant of vP_{max} and hP_{max} by influencing V_0, whereas the volume of specific lower limb muscles is the key determinant of P_{max} by influencing F_0.

Muscle fiber typology. In support of our hypotheses, univariable and multiple linear regression models showed that the muscle fiber typology of the GM explained a substantial magnitude of the variation of V_0 and P_{max} during both sprinting and jumping. There are several lines of evidence that support these findings derived directly from experiments on single muscle fibers and from studies using multijoint dynamic exercise. At a single fiber level, Bottinelli et al. (36) found that the maximum shortening velocity (i.e., V_0) and the P_{max} of Type II fibers were consistently higher than the Type I fibers from rat soleus, extensor digitorum longus, and plantaris muscles, as well as fibers from the human VL (37). Tihanyi et al. (38) demonstrated that well-trained jump athletes who possessed more than 50% Type II fibers in the VL were able to generate higher velocity, and more power, during knee extension exercise compared with athletes who possessed less than 50% Type II fibers. Furthermore, there were significant correlations between the percentage of Type II fibers and power, as well as velocity, at the four highest loads. In the present study, muscle fiber typology did not contribute to the multiple

TABLE 2. Lower limb muscle architecture, morphology, and fiber typology values.

Variable	Mean ± SD	Range
Muscle fiber typology (z-score)		
GM	–0.28 ± 1.04	–2.50 to 1.01
Muscle fascicle length (cm)		
GM	7.32 ± 1.15	5.39 to 10.20
GL	6.55 ± 0.97	5.00 to 9.46
VL	8.21 ± 0.62	7.27 to 9.52
BFLH	12.16 ± 1.29	9.75 to 14.46
Muscle thickness (cm)		
GM	1.48 ± 0.20	1.10 to 1.87
GL	1.78 ± 0.22	1.42 to 2.16
VL	2.77 ± 0.21	2.40 to 3.23
BFLH	2.66 ± 0.26	2.09 to 3.07
Pennation angle (°)		
GM	11.80 ± 1.42	8.51 to 14.21
GL	15.97 ± 1.51	12.90 to 18.44
VL	19.92 ± 2.06	17.40 to 23.93
BFLH	12.71 ± 1.27	10.84 to 15.71
Muscle volume (cm^3·kg-m)		
GMAX	7.21 ± 0.52	6.65 to 8.11
GMED	2.30 ± 0.28	1.78 to 2.82
GMIN	0.70 ± 0.15	0.37 to 0.93
TFL	0.57 ± 0.11	0.40 to 0.82
Sartorius	1.17 ± 0.29	0.78 to 1.95
Iliopsoas	2.72 ± 0.44	2.05 to 3.46
Gracilis	0.83 ± 0.10	0.65 to 1.08
ADD	8.63 ± 0.77	7.68 to 10.23
RF	2.15 ± 0.16	1.88 to 2.47
VL	5.17 ± 0.50	4.62 to 6.52
VI	3.52 ± 0.42	2.86 to 4.26
VM	4.04 ± 0.64	2.62 to 5.17
Semimembranosus	1.74 ± 0.29	1.13 to 2.25
Semitendinosus	1.68 ± 0.22	1.10 to 1.98
BFLH	1.72 ± 0.22	1.43 to 2.11
BFSH	0.83 ± 0.12	0.66 to 1.07
Soleus	2.85 ± 0.32	2.43 to 3.64
GM	1.76 ± 0.25	1.30 to 2.24
GL	1.08 ± 0.21	0.76 to 1.41
Total muscle volume	50.7 ± 2.7	44.6 to 56.9

TABLE 3. Pearson correlation values between the lower limb muscle characteristics and the mechanical variables derived from the horizontal (i.e., h) and vertical (i.e., v) FV and PV relationships.

Variable	hF_0 (N·kg^{-1})	hV_0 (m·s^{-1})	hP_{max} (W·kg^{-1})	vF_0 (N·kg^{-1})	vV_0 (m·s^{-1})	vP_{max} (W·kg^{-1})
Muscle fiber typology (*z*-score)						
GM	0.397	0.658**	0.669*	–0.111	0.762***	0.581**
Muscle fascicle length (cm)						
GM	–0.161	–0.186	–0.388	0.150	–0.156	–0.149
GL	0.257	–0.029	0.147	–0.124	–0.072	–0.219
VL	–0.496	–0.287	–0.170	–0.091	–0.139	–0.258
BFLH	0.229	0.546*	0.571*	0.023	0.291	0.486
Muscle thickness (cm)						
GM	0.482*	0.014	0.254	0.479*	0.059	0.089
GL	0.431*	0.138	0.312	–0.273	0.265	0.057
VL	–0.054	0.175	0.011	–0.095	0.040	0.053
BFLH	0.039	0.339	0.118	0.054	0.024	0.093
Pennation angle (°)						
GM	0.481*	0.275	0.343	–0.080	0.234	0.141
GL	0.166	0.191	0.209	–0.270	0.493*	0.343
VL	0.330	0.368	0.141	0.035	0.217	0.191
BFLH	–0.146	–0.094	–0.125	0.020	–0.313	–0.379
Muscle volume (cm^3·kg-m)						
GMAX	0.512*	–0.245	0.320	–0.412	0.287	–0.149
GMED	–0.219	–0.040	–0.164	0.115	–0.312	–0.223
GMIN	–0.034	–0.099	0.147	–0.126	0.111	0.015
TFL	0.376	0.169	0.491*	0.094	–0.051	0.011
Sartorius	0.531*	0.203	0.543*	–0.222	0.404	0.284
Iliopsoas	0.531*	0.397	0.598**	–0.135	0.351	0.254
Gracilis	–0.269	–0.247	0.163	–0.196	0.126	–0.087
Adductors	0.579**	0.513*	0.667**	0.541*	0.382	0.376
RF	0.495*	0.319	0.485*	0.544*	0.150	0.338
VL	0.184	0.062	0.125	0.548*	0.051	0.647**
VI	0.497*	–0.059	0.575*	0.501*	0.127	0.333
VM	0.544*	0.505*	0.600**	–0.044	0.311	0.344
Semimembranosus	0.033	–0.039	0.247	–0.255	0.158	–0.109
Semitendinosus	0.439	0.257	–0.267	0.255	–0.255	–0.115
BFLH	0.244	0.278	0.496*	0.135	0.227	0.431
BFSH	–0.192	0.678**	0.260	0.172	0.307	0.322
Soleus	0.381	0.383	0.300	0.154	0.199	0.325
GM	0.394	0.177	0.193	0.089	0.266	0.388
GL	–0.089	0.277	0.022	–0.112	0.164	0.177
Total muscle volume	0.555*	0.466	0.780***	0.229	0.440	0.489*

*$P < 0.05$.
**$P < 0.01$.
***$P < 0.001$.
hF_0, maximum horizontal force; hV_0, maximum horizontal velocity; hP_{max}, maximum horizontal power; vF_0, maximum vertical force; vV_0, maximum vertical velocity; vP_{max}, maximum vertical power.

linear regression models explaining the variation in vF_0 and hF_0 values. This finding is also supported by single fiber studies that indicate F_0 is not consistently different between fiber types (39,40). Based on previous research (15), and the findings from the present study, it is reasonable to suggest that possessing a higher proportion of Type II fibers would be beneficial for sprints of longer duration where athletes reach peak sprinting velocity. This hypothesis could be supported by the relationship between muscle fiber typology and mechanical variables underpinning sprint performance (i.e., hP_{max} and hV_0), given that these variables are strongly associated with sprints of longer duration (i.e., mean 100-m speed and 4-s sprinting distance) whereas hF_0 is not (41,42). During the latter stages of a sprint when maximal velocity is being approached, the short ground contact time and resultant contraction time does not allow for maximal muscle force to be reached (43), and the rate of force development is more important. During this stage of sprinting, possessing a higher estimated proportion of Type II fibers would promote the ability to continue to produce force at high velocities and achieve greater hV_0. Akin to single muscle fiber experiments, both Type IIa and Type IIx fibers can produce more force at higher shortening velocities than Type I fibers (37,39), which may underpin the association found in the present study between muscle fiber typology and hV_0. It should be noted that our estimation of muscle fiber typology in the GM likely reflects the typology of other prominent lower limb muscles. There appears to be an across-muscle phenotype, whereby individuals who express a high proportion of a given fiber type proportion in one muscle also express a comparably high proportion of the same fiber type in other muscles (44). Nonetheless, the measurement of muscle fiber typology in other lower limb muscles may have added value in the present study. Our findings demonstrate a clear advantage for athletes competing in explosive sports who possess fast muscle fiber typology.

Muscle volume. Given that muscle volume is a well-recognized determinant of its force-generating capacity (20), it was not surprising that we observed several lower limb muscles displaying a positive association with both hF_0 and vF_0. In further support of our hypotheses, the multiple linear regression models revealed that ADD volume and knee extensor muscles were key determinants of F_0 during both sprinting and jumping, thus influencing vP_{max} and hP_{max}. Although few studies have associated lower limb muscle volumes with mechanical

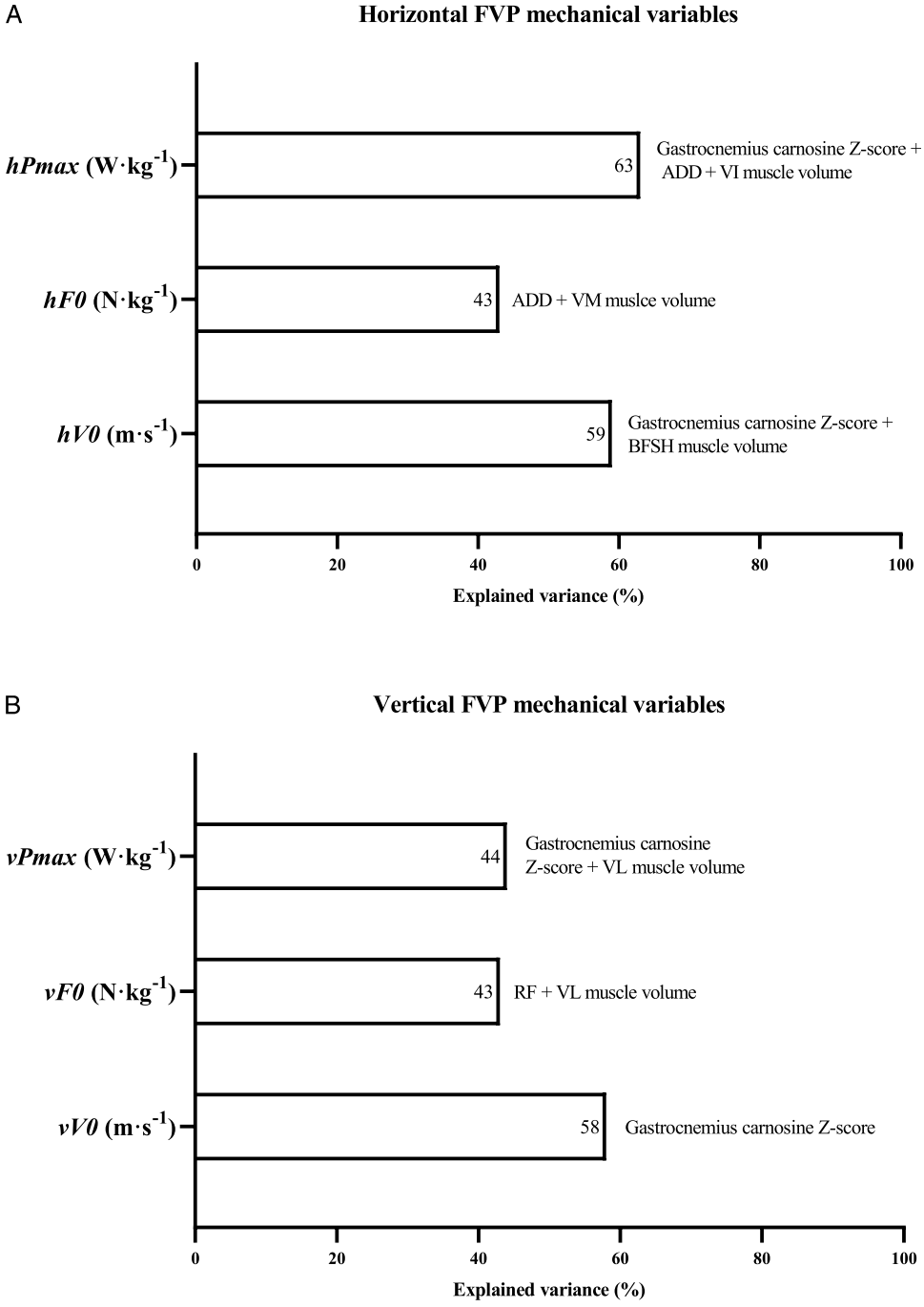

FIGURE 2—Determinants of the mechanical variables derived from the horizontal (A) and vertical FV and power–velocity profiles (B). Bars indicate the magnitude of explained variance (% r^2) obtained from multivariable linear regression analyses with the combination of predictors presented at the top of each bar. ADD, adductor magnus, longus, and brevis; hF_0, maximum horizontal force; hV_0, maximum horizontal velocity; hP_{max}, maximum horizontal power; vF_0, maximum vertical force; vV_0, maximum vertical velocity; vP_{max}, maximum vertical power.

variables from the horizontal FV and PV profiles directly, our findings agree with cross-sectional studies that have reported most hip and knee-crossing muscles to be significantly larger in sprinters compared with recreationally active individuals (11) and endurance runners (12). In particular, sprinters possess significantly larger VM (30%) and adductor magnus, longus, and brevis (22%–26%) muscles than nonsprinters when normalized to height and mass. More recent work (18) reported that hip extensor muscles were substantially larger (+32%) in elite (10.10 ± 0.07 s 100 m sprinters) compared with subelite sprinters (10.80 ± 0.30 s). Interestingly, this study (18) reported that GMAX alone explained 34%–44% of the variation in season best 100-m sprint performance. In agreement with this study and our hypothesis, we found that GMAX volume was significantly associated with hF_0, but it did not contribute to the multivariable regression model, whereby ADD and VM

TABLE 4. Stepwise linear regression model parameter estimates for the relationship between the vertical and the horizontal FV and PV mechanical variables (dependent variables) and muscle architecture (i.e., fascicle length, pennation angle and thickness), morphology (i.e., muscle volume), and fiber typology (gastrocnemius carnosine *z*-score).

Statistics	Horizontal F_0 (N·kg^{-1})	Horizontal V_0 (m·s^{-1})	Horizontal P_{max} (W·kg^{-1})	Vertical F_0 (N·kg^{-1})	Vertical V_0 (m·s^{-1})	Vertical P_{max} (W·kg^{-1})
Predictors	ADD[1] and VM volume[2]	GM *z*-score[1] and BFSH volume[2]	GM *z*-score[1] and VI[2] and ADD volume[3]	RF[1] and VL volume[2]	GM *z*-score[1]	GM *z*-score[1] and VL volume[2]
Adjusted r^2	0.432	0.590	0.634	0.430	0.580	0.440
P value	0.007	<0.001	0.001	0.008	<0.001	0.006
SEE	0.60	0.42	0.96	0.60	0.25	1.42
Variable 1						
Unstandardized coefficient (B)	0.53	0.31	0.62	0.51	0.16	0.87
SE	0.21	0.12	0.26	0.20	0.06	0.36
Standardized coefficient (Beta)	0.51	0.44	0.39	0.49	0.58	0.48
r^2 change	0.32	0.47	0.34	0.48	0.30	0.37
P value	0.020	0.025	0.032	0.012	0.009	0.030
Variable 2						
Unstandardized coefficient (B)	0.88	3.04	0.87	0.85		1.28
SE	0.39	1.09	0.34	0.38		0.64
Standardized coefficient (Beta)	0.44	0.50	0.40	0.43		0.40
r^2 change	0.18	0.16	0.14	0.15		0.11
P value	0.040	0.015	0.025	0.040		0.009
Variable 3						
Unstandardized coefficient (B)			1.41			
SE			0.60			
Standardized coefficient (Beta)			0.37			
r^2 change			0.11			
P value			0.035			

ADD, adductor magnus, longus, and brevis; F_0, theoretical maximal force; V_0, theoretical maximal velocity; P_{max}, theoretical maximal power.

volume explained the most variation in hF_0. In support, Sugisaki et al. (24) reported that variation in 30-m sprint running time was best explained by the anatomical CSA of the ADD. Given that we found the ADD to be a significant determinant of hF_0, it is probable that the ADD are important muscles for sprint acceleration. This importance may arise from the contribution of the ADD to hip extension torque during the late-swing to early contact phase of sprint acceleration (24). Adductor magnus acts as a hip extensor through the entire hip joint range of motion, whereas the adductor brevis and longus also act as hip extensors when the hip is flexed more than 25° and 50°, respectively (24,45). Furthermore, the high degrees of hip flexion experienced during acceleration may increase the mechanical effectiveness of adductor magnus and reduce the effectiveness of GMAX via alterations to moment arms (45). In addition to the ADD, the volume of the VM contributed to the regression model explaining variation in hF_0. Previous research has reported that maximal isokinetic knee extensor torque is negatively correlated with 15-m sprint time (46), whereby knee extensor torque is thought to contribute to the swing and stance phases during sprinting (25). These findings, along with those of the present study, highlight the important

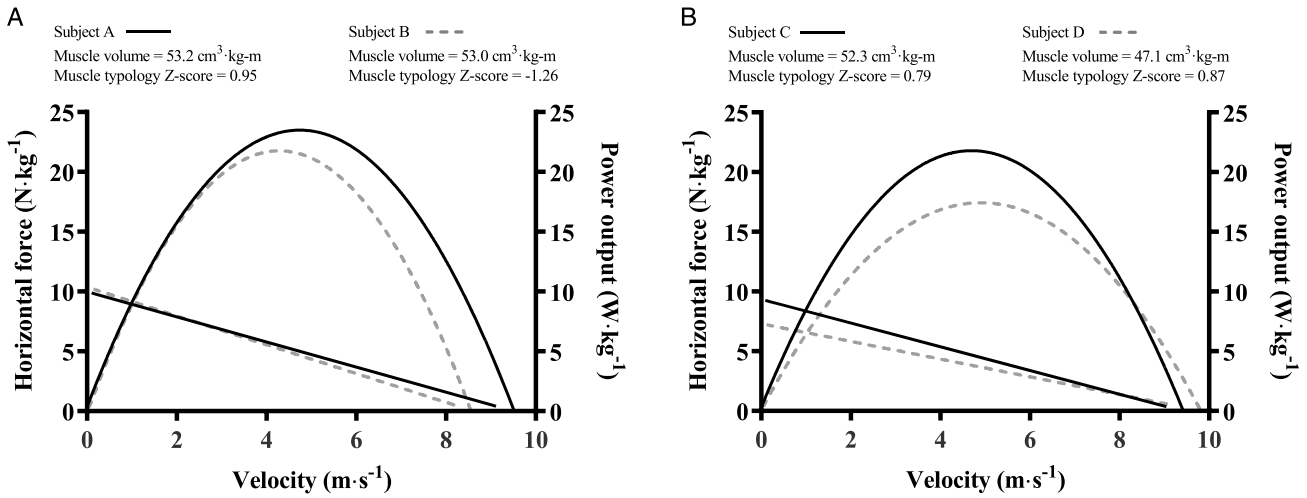

FIGURE 3—Typical traces of linear FV and second-degree polynomial PV relationships obtained from overground sprinting for subjects with similar lower limb muscle volume but divergent in muscle fiber typology (A; subjects A and B) and for subjects with similar muscle fiber typology but divergent in lower limb muscle volume (B; subjects C and D). Typically, subjects with a higher estimated proportion of Type II fibers (i.e., higher carnosine *z*-score) possessed greater hV_0 and hP_{max} (i.e., subject A) compared with those with a lower estimated proportion of Type II fibers. Subjects with greater lower limb muscle volume possessed greater hV_0 and hP_{max} compared with those with a smaller lower limb muscle volume. In particular, the volume of the ADD and VI (hP_{max}) and VM (hV_0) seemed to be most influential on the maximal mechanical parameters. ADD, adductor magnus, longus, and brevis; hF_0, maximum horizontal force; hP_{max}, maximum horizontal power.

role of the knee extensors during the acceleration phase of sprinting. We found that the volume of the BFSH significantly contributed to the regression model explaining the variation in hV_0 in sprinting. Previous research (47) has shown that a greater amount of horizontal force (averaged over an entire sprint acceleration) was found in subjects who had greater BF activation just before ground contact and superior eccentric hamstring torque. These findings show the important role that the BF has during sprint running. Future work should seek to determine whether interventions targeted at promoting hypertrophy in the muscles associated with the mechanical parameters underpinning the horizontal FV and PV profiles lead to an improvement in sprint acceleration. Lastly, in agreement with our hypotheses, we found that the volumes of plantar flexor muscles were not associated with variation in the mechanical parameters of the FV and PV profiles.

Muscle architecture. In the present study, muscle architecture only explained a small amount of variation in the maximal mechanical parameters of the horizontal or vertical FV or PV profiles. Specifically, univariable analyses revealed that BFLH fascicle length was associated with greater hV_0 and hP_{max}, whereas the thickness of the GL and GM were associated with hF_0 (GM and GL) and vF_0 (GM). These findings only partly agreed with out hypotheses, as we surmised that the fascicle length of all lower limb muscles that we measured would be associated with hV_0 and hP_{max}. Theoretically, muscles with longer fascicles, and presumably more sarcomeres in series, exhibit higher shortening velocities (when completely unloaded) and greater contractility than muscles with shorter fascicles (20). Consequently, longer fascicles within the BFLH may improve the rate at which the forward swinging lower limb is decelerated during the late-swing phase of sprinting, which may contribute to greater velocities via increasing stride frequency. Greater rates of BFLH shortening may also contribute to an enhanced hip extensor moment during sprinting and jumping. Although these hypotheses require further investigation, it is important to consider that fascicle lengths of the VL, GM, and GL were not associated with the mechanical variables of the vertical or horizontal FV and PV profiles in the current study. Recent work (21) reported that GM muscle fascicle length accounted for almost half of the difference in V_0 between young and old men derived from the plantarflexion torque–velocity relationship. However, in the current study, FV and PV profiles were determined during the multijoint, dynamic movements of sprinting and jumping compared with the torque–velocity relationships derived from single joint movements of the ankle dorsiflexors. Interestingly, studies from the same research group (10,14) reported longer GM, GL, and VL muscle fascicles in male sprinters (10) compared with distance runners and nonathletes, and in fast (10.0–10.9 s 100-m sprinters) compared with slow sprinters (11.0–11.7 s) (14). Furthermore, pennation angle (r = 0.34 to 0.46, $P < 0.05$) and muscle fascicle length (r = −0.40 to −0.54, $P < 0.05$) were associated with personal best 100-m times (14). These findings would suggest that these muscle architectural characteristics may underpin the mechanical variables from the horizontal FV and PV profile given their relationship to sprint performance (41,42). Despite this premise, we had a smaller sample size compared with these studies (10,14), other studies did not use measures of actual performance or mechanical variables (10), and it may not be appropriate to compare elite 100-m sprinters (10,14) with subelite rugby league athletes. Interestingly, we observed that greater thickness but not volume of the GM and GL muscles was associated with hF_0. Although this observation may be difficult to reconcile, it is consistent with previous work. For example, Abe et al. (10) and Kumagai et al. (14) both reported that sprint-trained athletes had thicker GL muscles than sedentary controls. However, Handsfield et al. (11) found no significant difference in GL (7%) or GM (4%) muscle volumes (normalized to body size) when comparing sprinters to nonsprinters. These data suggest the possibility that the muscle bellies of these muscles may be relatively short despite still having a large physiological CSA, but this notion requires further investigation. One previous study (22) has shown that quadriceps thickness and VL pennation angle explained ~62% of the variation in vF_0 estimated from loaded and unloaded countermovement jumps. Fiber pennation increases a muscle's physiological CSA (via increasing the number of sarcomeres in parallel), which is proportional to its force-generating capacity (20). As such, a greater pennation angle is likely to be associated with a greater volume of muscle. Although we did not observe any association between VL pennation angle or thickness and vF_0, which disagreed with our hypotheses, we did find that VL volume (along with RF) contributed to the regression model explaining ~43% of the variation in vF_0. Differences in the type of jump that was used (squat or countermovement jump), or the way in which muscle architecture was quantified, may have contributed to the lack of association that we found with the architecture of the VL in the present study compared with that of Morales-Artacho et al. (22). The latter study measured muscle thickness at the middle and proximal regions of the VM, VL, RF, and VI to provide a measure of mean quadriceps muscle thickness and pennation angle of the VL was taken as the average value from three sites (e.g., at 20%, 50%, and 60% of thigh length), while we relied on a single measurement site of the VL. Given that muscle thickness and pennation angle measurements vary along the length of the muscle, muscle architecture measurements at multiple sites within a muscle may be necessary to reduce some of the within-muscle variability. Nonetheless, given that the overall volume of a muscle is directly related to its force-generating capacity (20), our hypothesis was confirmed, whereby the volume of the knee extensor muscles can explain a substantial amount of the variability in vF_0 and vP_{max}.

Limitations. There are some limitations of this study that should be acknowledged. First, the ultrasound field of view could not capture the entire length of fascicles, and as a consequence, fascicle length was estimated using extrapolation methods (34). Although this estimation technique has been validated against cadaveric measurements (48), it was recently shown that this approach overestimated BFLH fascicle length when compared with extended field of view scans (49). At present, extended field of view imaging has not been validated against cadaveric data, so the current methodology should not

be considered inferior. The extrapolation methods used in the present study have high levels of interday reliability in our laboratory (ICC >0.95 and CV <6%) for muscle fascicle length measurements of the GM, GL, VL, and BFLH. Nonetheless, muscle architecture measures were only performed at a single location in four lower limb muscles, which may have limited the strength of the associations with horizontal and vertical FV and PV mechanical parameters compared with a previous study (22). Our estimation of muscle fiber typology is based on the ^{1}H-MRS measurement of muscle carnosine, which is a stable dipeptide that is present in twofold higher concentrations in Type II fibers and is positively correlated (P = 0.009 and r = 0.714) with the muscle biopsy determined proportion of Type II fibers (26). When this association is translated to explained variance (i.e., r^2), ~50% of the variability in muscle fiber typology (i.e., myosin heavy chain composition) is not explained by variation in muscle carnosine content. It should be noted that a large portion of this unexplained variation may be due to the lower levels of reliability of the methods used to determine myosin heavy chain composition given that we showed extremely high levels of reliability between interday ^{1}H-MRS measurements of muscle carnosine (CV = 4.3%). Indeed, a recent study (50) demonstrated that the interbiopsy variation (CV) in MHC Type I, Type IIa, and Type IIx fibers was 21.5%, 15.4%, and 42.0%, respectively. In addition, ^{1}H-MRS samples both superficial and deep parts of the muscle as well as a substantially larger volume of muscle compared with a muscle biopsy, which may also contribute to the unexplained variation between measurements. Lastly, we report a large number of correlation analyses, some of which fall outside the scope of our hypotheses, which may result in a type I error inflation, and so their interpretation should be done with caution.

Conclusions. This study demonstrates that lower limb muscle characteristics are associated with the mechanical parameters of the FV and PV profiles in subelite rugby league players. Muscle fiber typology and specific lower limb muscle volumes are major determinants of vP_{max} and hP_{max}, by influencing V_0 and F_0, respectively. Although muscle architectural characteristics did not seem to be as deterministic as other muscle characteristics, BFLH fascicle length was associated with greater hV_0 and hP_{max}, and the thickness of the GL and GM was associated with hF_0 and vF_0. These findings may inform the design of targeted training programs to maximize sprint and jump performance in athletes.

The authors declare that they received internal funding from Griffith University and external funding from the Gold Coast Titans rugby league club, which supported MR-related costs for the data collection. The authors also thank Dan Ferris and Joel Grech from the Gold Coast Titans rugby league club for facilitating this project. The authors have no competing interests to disclose. The results of the present study are presented clearly, honestly, and without fabrication and do not constitute endorsement by the American College of Sports Medicine.

REFERENCES

1. Kraemer WJ, Newton RU. Training for muscular power. *Phys Med Rehabil Clin N Am*. 2000;11(2):341–68.
2. Baker DG, Newton RU. Comparison of lower body strength, power, acceleration, speed, agility, and sprint momentum to describe and compare playing rank among professional rugby league players. *J Strength Cond Res*. 2008;22(1):153–8.
3. Samozino P, Rabita G, Dorel S, et al. A simple method for measuring power, force, velocity properties, and mechanical effectiveness in sprint running. *Scand J Med Sci Sports*. 2016;26(6):648–58.
4. Morin JB, Samozino P. Interpreting power–force–velocity profiles for individualized and specific training. *Int J Sports Physiol Perform*. 2016;11(2):267–72.
5. Samozino P, Morin J-B, Hintzy F, Belli A. A simple method for measuring force, velocity and power output during squat jump. *J Biomech*. 2008;41(14):2940–5.
6. Ingalls CP. Nature vs. nurture: can exercise really alter fiber type composition in human skeletal muscle? *J Appl Physiol*. 2004;97(5):1591–2.
7. Seynnes OR, de Boer M, Narici MV. Early skeletal muscle hypertrophy and architectural changes in response to high-intensity resistance training. *J Appl Physiol (1985)*. 2007;102(1):368–73.
8. Jiménez-Reyes P, Samozino P, Brughelli M, Morin JB. Effectiveness of an individualized training based on force–velocity profiling during jumping. *Front Physiol*. 2017;7:677.
9. Jiménez-Reyes P, Samozino P, García-Ramos A, Cuadrado-Peñafiel V, Brughelli M, Morin JB. Relationship between vertical and horizontal force–velocity–power profiles in various sports and levels of practice. *PeerJ*. 2018;6:e5937.
10. Abe T, Kumagai K, Brechue WF. Fascicle length of leg muscles is greater in sprinters than distance runners. *Med Sci Sports Exerc*. 2000;32(6):1125–9.
11. Handsfield GG, Knaus KR, Fiorentino NM, Meyer CH, Hart JM, Blemker SS. Adding muscle where you need it: non-uniform hypertrophy patterns in elite sprinters. *Scand J Med Sci Sports*. 2017;27(10):1050–60.
12. Bex T, Iannaccone F, Stautemas J, et al. Discriminant musculo-skeletal leg characteristics between sprint and endurance elite Caucasian runners. *Scand J Med Sci Sports*. 2017;27(3):275–81.
13. Chelly MS, Chérif N, Amar MB, et al. Relationships of peak leg power, 1 maximal repetition half back squat, and leg muscle volume to 5-m sprint performance of junior soccer players. *J Strength Cond Res*. 2010;24(1):266–71.
14. Kumagai K, Abe T, Brechue WF, Ryushi T, Takano S, Mizuno M. Sprint performance is related to muscle fascicle length in male 100-m sprinters. *J Appl Physiol*. 2000;88(3):811–6.
15. Mero A. Relationships between the maximal running velocity, muscle fiber characteristics, force production and force relaxation of sprinters. *Scand J Sports Sci*. 1981;3:16–22.
16. Methenitis SK, Zaras ND, Spengos KM, et al. Role of muscle morphology in jumping, sprinting, and throwing performance in participants with different power training duration experience. *J Strength Cond Res*. 2016;30(3):807–17.
17. Earp JE, Joseph M, Kraemer WJ, et al. Lower-body muscle structure and its role in jump performance during squat, countermovement, and depth drop jumps. *J Strength Cond Res*. 2010;24(3):722–9.
18. Miller R, Balshaw TG, Massey GJ, et al. The muscle morphology of elite sprint running. *Med Sci Sports Exerc*. 2021;53(4):804–15.
19. Bosco C, Komi PV. Mechanical characteristics and fiber composition of human leg extensor muscles. *Eur J Appl Physiol*. 1979;41(4):275–84.
20. Lieber RL, Fridén J. Functional and clinical significance of skeletal muscle architecture. *Muscle Nerve*. 2000;23(11):1647–66.
21. Thom JM, Morse CI, Birch KM, Narici MV. Influence of muscle architecture on the torque and power–velocity characteristics of young and elderly men. *Eur J Appl Physiol*. 2007;100(5):613–9.
22. Morales-Artacho AJ, Ramos AG, Pérez-Castilla A, et al. Associations of the force–velocity profile with isometric strength and neuromuscular factors. *Int J Sports Med*. 2018;39(13):984–94.

23. Takahashi K, Wakahara T. Association between trunk and gluteus muscle size and long jump performance. *PloS One*. 2019;14(11): e0225413.
24. Sugisaki N, Kanehisa H, Tauchi K, Okazaki S, Iso S, Okada J. The relationship between 30-m sprint running time and muscle cross-sectional areas of the psoas major and lower limb muscles in male college short and middle distance runners. *Int J Sport Health Sci*. 2010; 1101140066.
25. Delecluse C. Influence of strength training on sprint running performance. *Sports Med*. 1997;24(3):147–56.
26. Baguet A, Everaert I, Hespel P, Petrovic M, Achten E, Derave W. A new method for non-invasive estimation of human muscle fiber type composition. *PloS One*. 2011;6(7):e21956.
27. Samozino P, Rejc E, Di Prampero PE, Belli A, Morin JB. Optimal force–velocity profile in ballistic movements—altius: citius or fortius? *Med Sci Sports Exerc*. 2012;44(2):313–22.
28. Haugen T, Buchheit M. Sprint running performance monitoring: methodological and practical considerations. *Sports Med*. 2016;46(5): 641–56.
29. Hamner SR, Seth A, Delp SL. Muscle contributions to propulsion and support during running. *J Biomech*. 2010;43(14):2709–16.
30. Jacobs R, Bobbert MF, van Ingen Schenau GJ. Mechanical output from individual muscles during explosive leg extensions: the role of biarticular muscles. *J Biomech*. 1996;29(4):513–23.
31. MacMillan EL, Bolliger CS, Boesch C, Kreis R. Influence of muscle fiber orientation on water and metabolite relaxation times, magnetization transfer, and visibility in human skeletal muscle. *Magn Reson Med*. 2016;75(4):1764–70.
32. Bellinger P, Desbrow B, Derave W, et al. Muscle fiber typology is associated with the incidence of overreaching in response to overload training. *J Appl Physiol*. 2020;129:823–836.
33. Timmins RG, Ruddy JD, Presland J, et al. Architectural changes of the biceps femoris long head after concentric or eccentric training. *Med Sci Sports Exerc*. 2016;48(3):499–508.
34. Fukunaga T, Ichinose Y, Ito M, Kawakami Y, Fukashiro S. Determination of fascicle length and pennation in a contracting human muscle in vivo. *J Appl Physiol*. 1997;82(1):354–8.
35. Lund H, Christensen L, Savnik A, Boesen J, Danneskiold-Samsøe B, Bliddal H. Volume estimation of extensor muscles of the lower leg based on MR imaging. *Eur Radiol*. 2002;12(12):2982–7.
36. Bottinelli R, Schiaffino S, Reggiani C. Force–velocity relations and myosin heavy chain isoform compositions of skinned fibres from rat skeletal muscle. *J Physiol*. 1991;437(1):655–72.
37. Bottinelli R, Canepari M, Pellegrino MA, Reggiani C. Force–velocity properties of human skeletal muscle fibres: myosin heavy chain isoform and temperature dependence. *J Physiol*. 1996;495(2):573–86.
38. Tihanyi J, Apor P, Fekete G. Force–velocity–power characteristics and fiber composition in human knee extensor muscles. *Eur J Appl Physiol*. 1982;48(3):331–43.
39. Widrick JJ, Trappe SW, Costill DL, Fitts RH. Force–velocity and force–power properties of single muscle fibers from elite master runners and sedentary men. *Am J Physiol Cell Physiol*. 1996;271(2): C676–83.
40. Schiaffino S, Reggiani C. Fiber types in mammalian skeletal muscles. *Physiol Rev*. 2011;91(4):1447–531.
41. Morin J-B, Bourdin M, Edouard P, Peyrot N, Samozino P, Lacour J-R. Mechanical determinants of 100-m sprint running performance. *Eur J Appl Physiol*. 2012;112(11):3921–30.
42. Morin J-B, Edouard P, Samozino P. Technical ability of force application as a determinant factor of sprint performance. *Med Sci Sports Exerc*. 2011;43(9):1680–8.
43. Andersen LL, Aagaard P. Influence of maximal muscle strength and intrinsic muscle contractile properties on contractile rate of force development. *Eur J Appl Physiol*. 2006;96(1):46–52.
44. Vikne H, Gundersen K, Liestøl K, Mælen J, Vøllestad N. Intermuscular relationship of human muscle fiber type proportions: slow leg muscles predict slow neck muscles. *Muscle Nerve*. 2012;45(4): 527–35.
45. Dostal WF, Soderberg GL, Andrews JG. Actions of hip muscles. *Phys Ther*. 1986;66(3):351–9.
46. Dowson MN, Nevill ME, Lakomy HK, Nevill AM, Hazeldine RJ. Modelling the relationship between isokinetic muscle strength and sprint running performance. *J Sports Sci*. 1998;16(3):257–65.
47. Morin JB, Gimenez P, Edouard P, et al. Sprint acceleration mechanics: the major role of hamstrings in horizontal force production. *Front Physiol*. 2015;6:404.
48. Kellis E, Galanis N, Natsis K, Kapetanos G. Validity of architectural properties of the hamstring muscles: correlation of ultrasound findings with cadaveric dissection. *J Biomech*. 2009;42(15):2549–54.
49. Franchi MV, Fitze DP, Raiteri BJ, Hahn D, Spörri J. Ultrasound-derived biceps femoris long head fascicle length: extrapolation pitfalls. *Med Sci Sports Exerc*. 2020;52(1):233–43.
50. Sahl RE, Morville T, Kraunsøe R, Dela F, Helge JW, Larsen S. Variation in mitochondrial respiratory capacity and myosin heavy chain composition in repeated muscle biopsies. *Anal Biochem*. 2018;556: 119–24.